DNA Methylation–Dependent Restriction of Tyrosine Hydroxylase Contributes to Pancreatic β-Cell Heterogeneity

Nazia Parveen,[1] Jean Kimi Wang,[1] Supriyo Bhattacharya,[2] Janielle Cuala,[3] Mohan Singh Rajkumar,[4] Alexandra E. Butler,[5] Xiwei Wu,[2] Hung-Ping Shih,[1] Senta K. Georgia,[6,7] and Sangeeta Dhawan[1]

Diabetes 2023;72:575–589 | https://doi.org/10.2337/db22-0506

The molecular and functional heterogeneity of pancreatic β-cells is well recognized, but the underlying mechanisms remain unclear. Pancreatic islets harbor a subset of β-cells that co-express tyrosine hydroxylase (TH), an enzyme involved in synthesis of catecholamines that repress insulin secretion. Restriction of the TH$^+$ β-cells within islets is essential for appropriate function in mice, such that a higher proportion of these cells corresponds to reduced insulin secretion. Here, we use these cells as a model to dissect the developmental control of β-cell heterogeneity. We define the specific molecular and metabolic characteristics of TH$^+$ β-cells and show differences in their developmental restriction in mice and humans. We show that TH expression in β-cells is restricted by DNA methylation during β-cell differentiation. Ablation of de novo DNA methyltransferase Dnmt3a in the embryonic progenitors results in a dramatic increase in the proportion of TH$^+$ β-cells, whereas β-cell–specific ablation of Dnmt3a does not. We demonstrate that maintenance of *Th* promoter methylation is essential for its continued restriction in postnatal β-cells. Loss of *Th* promoter methylation in response to chronic overnutrition increases the number of TH$^+$ β-cells, corresponding to impaired β-cell function. These results reveal a regulatory role of DNA methylation in determining β-cell heterogeneity.

Pancreatic islets comprise several cell types, including the insulin-producing β-cells, which collectively regulate glucose homeostasis. β-Cells display molecular and functional heterogeneity, with unique β-cell subpopulations characterizing specific developmental and disease contexts to subserve robust systemic adaptation to changing physiological demands (1,2). All pancreatic endocrine cell types, including the different β-cell subpopulations, originate from a common progenitor. Spatiotemporal cues during development modify and restrict progenitor gene expression profiles to drive differentiation and generate cellular heterogeneity. However, we have a limited understanding of the mechanisms that orchestrate differential gene expression underlying β-cell heterogeneity.

Epigenetic mechanisms, such as DNA methylation, mediate context-specific changes in gene expression to direct the progressive refinement of cell fates during development (3). DNA methylation is the best-studied epigenetic module, with the de novo DNA methyltransferases Dnmt3a and Dnmt3b establishing new methylation patterns, whereas Dnmt1 maintains and propagates existing patterns through cell division (4). Modulation of DNA methylation patterns is known to dictate cell fate choices. In pancreas, maintenance methylation by Dnmt1 is essential for the survival of pancreatic progenitors during embryonic development (5) and for maintaining β-cell identity in postnatal life (6). Restriction of Dnmt1 expression also contributes to lineage commitment bias within the endocrine progenitor pool (7). Much less is known about the contribution of new methylation patterns in endocrine specification and lineage restriction.

[1]Department of Translational Research and Cellular Therapeutics, Arthur Riggs Diabetes and Metabolism Research Institute, City of Hope, Duarte, CA
[2]Integrative Genomics Core, City of Hope, Duarte, CA
[3]Medical Biophysics Program, Keck School of Medicine, University of Southern California, Los Angeles, CA
[4]School of Computational and Integrative Sciences, Jawaharlal Nehru University, New Delhi, India
[5]Research Department, Royal College of Surgeons in Ireland Bahrain, Adliya, Bahrain
[6]Department of Pediatrics, Keck School of Medicine, University of Southern California, Los Angeles, CA
[7]Center for Endocrinology, Diabetes, and Metabolism, The Saban Research Institute, Children's Hospital Los Angeles, Los Angeles, CA

Corresponding author: Sangeeta Dhawan, sdhawan@coh.org

Received 2 June 2022 and accepted 3 January 2023

This article contains supplementary material online at https://doi.org/10.2337/figshare.21809586.

N.P. and J.K.W. contributed equally to this work.

See accompanying article, p. 557.

Dnmt3a is a part of the Nkx2.2 repressor complex that directs β-cell specification and is also essential for β-cell maturation in postnatal life (8,9). This suggests that de novo DNA methylation is important in refining cell fate choices during differentiation.

Here, we focus on a unique β-cell subpopulation as a paradigm to illustrate the contribution of DNA methylation in guiding endocrine lineage choices and heterogeneity. Pancreatic islets harbor a small number of β-cells that express the enzyme tyrosine hydroxylase (TH), which is a signature of sympathetic neurons. TH catalyzes the rate-limiting step in the synthesis of catecholamines that inhibit insulin secretion (10,11). Restriction of the TH^+ β-cells within islets is essential for appropriate insulin secretion in mice, such that mouse strains with a larger number of TH^+ β-cells have blunted insulin secretion (12). However, to our knowledge, there have been no systematic studies defining the molecular characteristics of these cells, nor do we know the mechanisms that restrict the TH^+ β-cells in islets. We demonstrate the essential requirement of DNA methylation in establishing endocrine cell heterogeneity during differentiation, using TH^+ β-cells as a model. We establish that the TH^+ islet cells coexpressing insulin represent a bona fide replication-competent β-cell subtype with distinct molecular and metabolic characteristics and display species-specific developmental profiles in mice and humans. Using developmental stage–specific ablation of DNA methyltransferases, we demonstrate that DNA methylation establishes the restriction of TH expression in β-cells during the transition from endocrine progenitors to β-cells and maintains it subsequently. We show that loss of *Th* promoter methylation leads to increased TH expression and impaired β-cell identity in response to chronic overnutrition. Our data establish an essential role for DNA methylation patterning in endocrine lineage determination toward generation of β-cell heterogeneity.

RESEARCH DESIGN AND METHODS

Human Pancreatic Samples

Pancreatic sections from human fetal (n = 1), neonatal (n = 3), and adult nondiabetic donors (n = 5) were procured from brain-dead organ donors by the Network for Pancreatic Organ Donors with Diabetes, University of Florida at Gainesville. Human fetal pancreas (n = 1; 16 weeks postconception) was obtained through the Terminal Tissue Bank at the University of Southern California. The investigators were given 4-μm pancreatic sections from each donor (deidentified). Sample characteristics are described in Supplementary Table 1.

Animals

All animal experiments were performed according to protocols approved by the Institutional Animal Care and Use Committee at City of Hope, University of Southern California, and University of California, Los Angeles. Mice were maintained on a C57BL/6J background. $Dnmt3a^{fl/fl}$ and $Dnmt1^{fl/fl}$ mice have been described (13,14). We used *Pdx1*-Cre (15) and *Ngn3*-Cre (16) mice to ablate Dnmts in the pancreatic and endocrine progenitors, respectively, and *Ins1*-Cre^{Thor} (17) for β-cell–specific deletion. The Cre lines harbored Rosa26R-*YFP* or Rosa26R-mTmG lineage reporters (18). We used *Pdx1*-Cre:Rosa26R-*YFP* and heterozygous Ngn3-EGFP embryos (19) to sort pancreatic and endocrine progenitors, respectively. Transgenic mice expressing mouse *Ins1* promoter (*MIP-GFP*) (20) were used to sort β-cells. Mice were fed ad libitum and kept under a 12-h light/dark cycle. Male and female mice were used for all studies except the high-fat diet (HFD) studies. For the HFD studies, 1.5-month-old male C57BL/6J mice (n = 8/group) were fed a control diet (CD; 10% calories from fat; Research Diets D12450B), or a HFD (55% calories from fat; Envigo TD.93075) for a short term (8 weeks) or long term (16 weeks).

Immunostaining, Imaging, and Morphometry

A standard immunofluorescence protocol was used to detect various proteins in pancreatic sections, as previously described (21,22). Primary antibodies were diluted in the blocking solution, as noted in Supplementary Table 2. Donkey- and goat-derived secondary fluorescent antibodies (Jackson ImmunoResearch) were diluted 1:200. Antifade mounting medium with DAPI was used to label nuclei (Vector Laboratories). Slides were viewed using a Leica DM6000 or DM6 B microscope (Leica Microsystems) and imaged using OpenLab (Improvision) or Leica Application Suite X (Leica). Confocal imaging was done on a Zeiss LSM 800 with AiryScan using ZEN software. To quantify TH^+ cells, all islets were imaged and the total numbers of $insulin^+$, TH^+, and TH^+–$insulin^+$ cells were manually counted. The data were expressed either as percentage of total TH^+ cells, or β-cells and islet cells. Senescence associated β-galactosidase (SA-β-gal) staining was performed at pH 6.0 using the Cell Signaling kit (catalog 9860), followed by immunofluorescent staining for TH and insulin. Quantification of replication (and senescence) in different subpopulations was done as described by Rodnoi et al. (22). We counted a minimum of 1,500 cells for adults and 700 cells for neonates. β-Cell mass was measured per our published protocol (21). Briefly, pancreatic sections spanning every 80 μm were stained for insulin, counterstained with hematoxylin-eosin, and scanned using a Leica DM6 B microscope. Images were processed using ImageJ (National Institutes of Health), and β-cell mass was calculated as a ratio of $insulin^+$ area to total pancreas area, multiplied by dry pancreas weight. Fluorescence Lifetime Imaging Microscopy (FLIM) was performed on an SP8 DIVE FALCON multiphoton microscope (Leica Microsystems) using a ×40/1.10 numerical aperture water-immersion objective (see Supplementary Methods).

Islets and Cell Sorting

Islets were isolated from mouse pancreas using perfusion with the Liberase enzyme blend (Sigma Aldrich), as described (21). For cell sorting, pancreatic buds from

Pdx1-Cre:Rosa26R-*YFP* embryos, heterozygous Ngn3-EGFP embryos, or the MIP-GFP transgenic pups were harvested and digested into single cells using TrypLE Express (ThermoFisher). Cells were sorted for green fluorescent protein imaging using a BD FACS Aria II to an average percentage purity of 85–95%, with wild-type cells being the negative control for FACS gating (9).

Physiology

Intraperitoneal glucose tolerance tests were performed as previously described (21,22). Briefly, mice were fasted overnight and were injected intraperitoneally with 2 mg/kg D-glucose in sterile 1× PBS. Blood glucose levels were measured immediately before injection (0 min) and then at 15, 30, 60, 90, and 120 min after injection. Glucose-stimulated insulin secretion (GSIS) was assessed using a static incubation assay, per our previous studies (9). For TH inhibition, freshly isolated islets were cultured for 24 h in the presence of 10 μmol/L α-methyl-*para*-tyrosine (AMPT; Sigma-Aldrich) or vehicle (1× PBS) and used for GSIS. Ins in supernatants and islet extracts was measured by ELISA (Mercodia).

Chromatin Immunoprecipitation, DNA Methylation, and mRNA Expression

Chromatin immunoprecipitation (ChIP) was carried out on sorted cells using a low-cell-number protocol (6,9), using 2.5 μg of antibody. The antibodies and primers used for ChIP are listed in Supplementary Tables 3 and 4. Bisulfite conversion of DNA from sorted cells and islets and sequencing of the converted DNA were performed according to our published methods (6,9) using primers described in Supplementary Table 5. We analyzed 20–25 independent clones per group; each experiment was repeated in biological triplicates. RNA extraction and quantitative real-time RT-PCR was performed as published (22) using primers listed in Supplementary Table 6.

Single-Cell RNA-Sequencing Analysis

Single-cell RNA-sequencing (scRNA-seq) analysis was performed on publicly available scRNA-seq data sets (n = 3) from islets of mice fed a low-fat diet (accession no. GSE12512; ref. 23), as described in Supplementary Methods.

Statistics

All data are expressed as mean ± SE. Mean and SEM values were calculated from at least triplicates (biological) of a representative experiment. The statistical significance of differences was measured by an unpaired Student t test for experiments with two groups and a continuous outcome; a one-way ANOVA with Šídák, Bonferroni, or Fisher least significant difference post hoc tests was used for experiments with repeat measures. $P < 0.05$ indicated statistical significance. In figures, asterisks indicate P values as follows: $*P < 0.05$, $**P < 0.01$, $***P < 0.005$, and $****P < 0.001$.

Data and Resource Availability

All data are available in the article or supplementary materials. Data sets and resources are available from the corresponding author upon reasonable request.

RESULTS

TH$^+$ Islet Cells Co-expressing Insulin Represent a Bona Fide β-Cell Subtype

Islet cells that co-express the enzyme TH have been described before (24), though their precise molecular identity remains obscure. TH expressing islet cells were readily detectable in adult wild-type mice, the majority of which co-expressed insulin (Fig. 1*A–C*). These β-cells had variable TH levels and frequently appeared as clusters (Fig. 1*B*). There was no overlap between TH and glucagon in adult islets, whereas TH was present in few adult δ-cells (Supplementary Fig. 1*A–C*). TH expression in β-cells was first observed at embryonic day (E) 15.5, prior to which TH was restricted to α-cells (Supplementary Fig 1*D*). We confirmed the endocrine and β-cell lineage identities of the islet-resident TH-expressing cells by using endocrine-specific (*Ngn3*-Cre:*R26R-mTmG*) and β-cell–specific (*Ins1*-Cre:*R26R-YFP*) lineage reporters and by colocalization of TH with the endocrine marker chromogranin A (Fig. 1*D*, Supplementary Fig. 1*E* and *F*). TH$^+$ β-cells expressed Glut2, maturity marker Ucn3, and β-cell transcription factors Pdx1, Nkx6.1, MafA, and NeuroD, similar to other β-cells (Fig. 1*E–G*, Supplementary Fig. 1G). Because TH also marks sympathetic neurons that are intimately linked to islet vasculature (25), we examined the interaction of TH$^+$ β-cells with sympathetic neurons and vasculature. These cells had greater contact with the Tuj1$^+$ sympathetic fibers and PECAM1$^+$ capillaries, compared with TH$^-$ β-cells (Fig. 1*H–J*, Supplementary Fig. 1*H–L*, Supplementary Movies 1 and 2). Prior work showed an inverse correlation between TH$^+$ β-cell number and islet function (12). Accordingly, TH inhibition in mouse islets using AMPT led to improved GSIS (Supplementary Fig. 1*M*).

TH$^+$ β-Cells Exist in the Developing Human Pancreas

To determine if TH$^+$ β-cells exist in humans, we mined two publicly available human islet scRNA-seq data analyses (26,27) and found that no more than 1% of adult human β-cells express *TH* at very low levels (Fig. 2*A*, Supplementary Fig. 2*A–E*). A histological survey of adult human pancreases did not show any TH$^+$ β-cells in the samples analyzed (0% of 2,000 β-cells per sample, n = 3) (Fig. 2*B* and *D*), regardless of the islet size, confirming their rarity in adult humans (Fig. 2*B*). Next, we examined TH expression in fetal and neonatal human pancreases. Although most islet structures lacked TH, small endocrine-cell clusters frequently harbored brightly stained TH$^+$ β-cells (Fig. 2*C* and *D*, Supplementary Fig. 2*F–I*). To confirm the developmental regulation of TH, we queried the β-Cell Hub and Broad Institute Single Cell Portal databases for single-cell transcriptomic comparison of the immature and mature human β-cell states modeled by

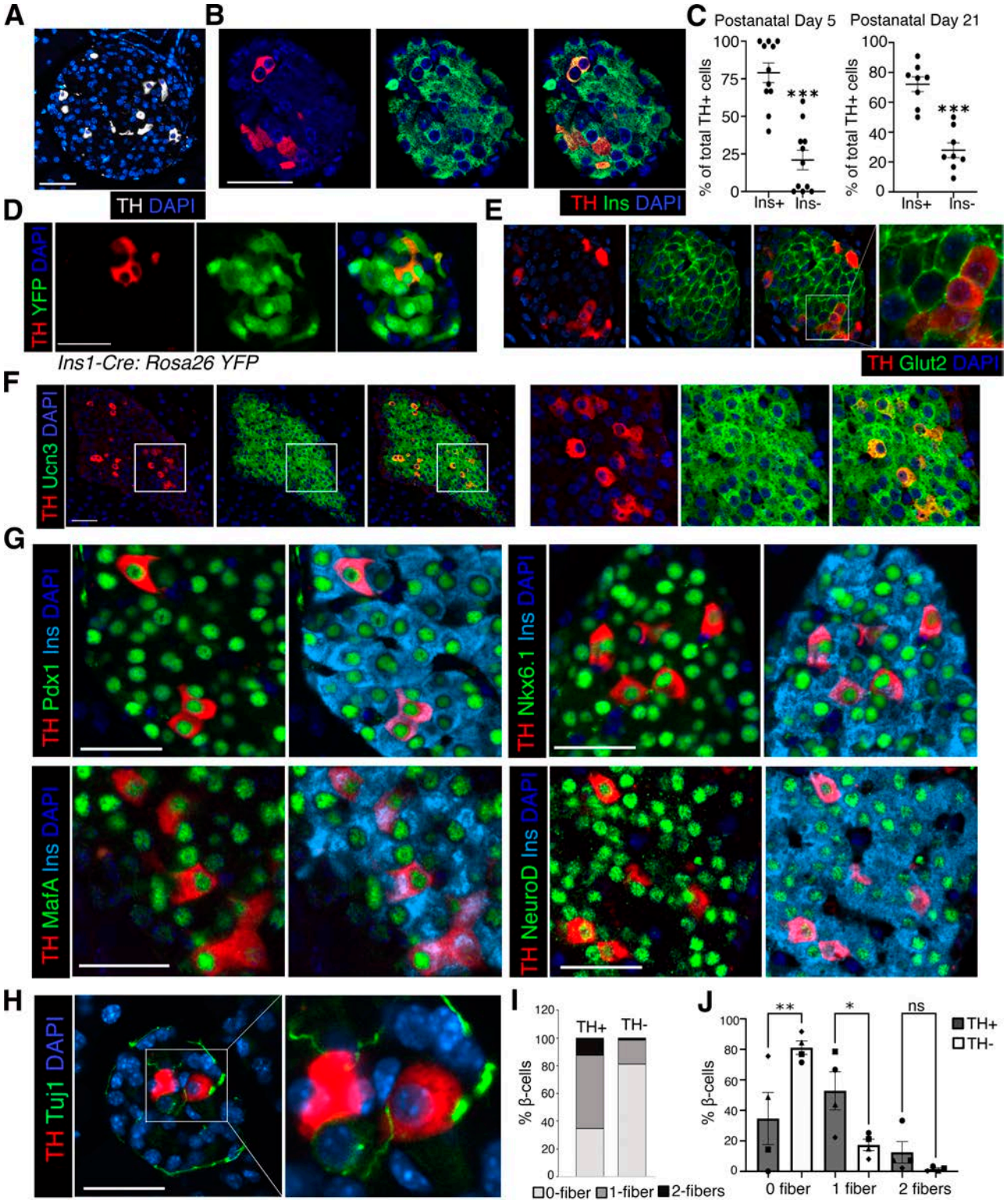

Figure 1—TH$^+$ islets cells co-expressing insulin (Ins) represent a bona fide β-cell subpopulation. *A* and *B*: Immunostaining for TH (gray) (*A*); TH (red) and insulin (green) (*B*); and DAPI (blue). *C*: Quantification of TH$^+$ cells assessed for insulin expression (shown as percentage of total TH$^+$ cells) at P5 (left panel: n = 700 β-cells/pancreas, n = 11 pancreas) and P21 (right panel: n = 1,200 β-cells per pancreas, n = 8 pancreas). *D*: Representative images from *Ins1*-Cre:*Rosa26* YFP mice (2 months old) stained for TH (red), yellow fluorescent protein (YFP; green), and DAPI (blue). *E* and *F*: Immunostaining for TH (red) with Glut2 (green) (*E*) or Urocortin3 (Ucn3; green) (*F*), and DAPI (blue). The far right panel in *E* and the three right panels in *F* show a ×2.5 magnification of the area marked by a white square. *G*: Immunostaining for TH (red), Pdx1/Nkx6.1/MafA/NeuroD1 (green), with DAPI (blue). *H*: Immunostaining for TH (red) with Tuj1 (green). Right panel is a ×2.5 magnification of the area in the white box. *I* and *J*: Quantification of Tuj1 plus fiber contact with TH$^+$ and TH$^-$ β-cells (n = 2,000 β-cells per slide, two slides spanning 100 μm for each pancreas, n = 4 pancreas), showing percentages of contact with none, one, or two fibers (*I*),

stem-cell derived β-like (sc-β-like; early/immature and late/mature) cells and human islet origin β-cells (28,29). Our queries showed higher *TH* expression in the sc-β-like cells compared with islet-derived β-cells (Fig. 2*E* and *F*) and revealed that Rho-associated protein kinase (ROCK) inhibitor treatment, which promotes the maturation of sc-β-like cells (30), led to a fivefold reduction in *TH* mRNA (Fig. 2*F*). These data suggest that reduced TH levels mark the human β-cell maturation process.

TH$^+$ β-Cells Are Transcriptionally and Metabolically Distinct

To define the unique molecular features of TH$^+$ β-cells, we meta-analyzed publicly available islet scRNA-seq data from adult C57BL/6J mice (23). All samples were integrated into one data set, and various cell types were identified by their standard gene signatures (Fig. 3*A*, Supplementary Fig. 3*A* and *B*). β-Cells were grouped into *Th*$^+$ and *Th*$^-$ categories; three of four β-cell clusters (clusters 0, 2, and 3) were enriched in *Th,* with ∼5% cells expressing high levels (Fig. 3*B*). Next, we surveyed for differentially expressed genes (DEGs) between the *Th*$^+$ and *Th*$^-$ β-cells and identified 130 such genes (Fig. 3*C*). The top enriched genes in the *Th*$^+$ group were *Mt1*, *Ftl1*, *Selenow*, *Mt2*, and *mt-Nd3*, whereas *Fkbp11*, *Manf*, *Pcsk1*, *Txnip*, *Pdia6*, and *Ero1lb* represented top downregulated genes. Gene-set enrichment analysis of these DEGs showed enrichment of pathways associated with protein synthesis, ribosomes, energy production, and ATP metabolism and downregulation of endoplasmic reticulum (ER) protein transport and ER stress response pathways (Fig. 3*D*, Supplementary Fig. 3*C*), hallmarks of ER stress and high oxidative phosphorylation (OxPhos).

To validate these findings, we first determined the metabolic characteristic of the TH$^+$ β-cells. We leveraged a FLIM method we developed to measure NADH levels in fixed tissue as a proxy of cellular metabolic status (31). FLIM measures the lifetime of excited NADH; unbound NADH exhibits short lifetimes and is a byproduct of glycolysis, whereas enzyme-bound NADH exhibits an ∼10× longer lifetime and is a substrate of OxPhos (32). We used immunofluorescence to identify TH$^+$ and TH$^-$ β-cells and collected their fluorescence intensity and NADH autofluorescent lifetimes. Comparison of average lifetimes for TH$^+$ and TH$^-$ β-cells (n = 8 islets per pancreas; n = 4 mice) showed a higher lifetime for TH$^+$ β-cells, indicating more oxidative metabolism (Fig. 3*E*, Supplementary Fig. 3*D*). We plotted the NADH intensity of each pixel of a TH$^+$ and TH$^-$ β-cell in an islet onto a phasor plot and determined the coordinates of the mode of NADH intensity for individual islets. We then plotted the average of those modes of all islets per animal on a *G* versus *S* axis (i.e., horizontal and vertical components, respectively, of lifetime measurements in arbitrary units) (Fig. 3*F*). The TH$^+$ β-cells clustered together to the left, implying more OxPhos (Fig. 3*F*). Next, we tested islet levels of *Ero1lb*-encoded endoplasmic reticulum oxidoreductase 1 beta (Ero1b), which catalyzes disulfide bond formation in the ER, is critical for insulin biogenesis, and protects from ER stress (33,34). Immunostaining confirmed scRNA-seq findings that, indeed, Ero1b was less abundant in TH$^+$ β-cells (Fig. 3*G*).

TH$^+$ β-Cells Can Replicate During Postnatal Life

It was previously proposed that TH$^+$ β-cells represent a senescent population that does not replicate (10). Replication is the primary mechanism for the growth and maintenance of β-cell mass in postnatal life, with rapid replication in neonatal life followed by gradual, age-dependent decline (21,35). Therefore, we examined the growth and replication of TH$^+$ β-cells in postnatal life. To establish their growth profile, we quantified TH$^+$ β-cells in wild-type murine pancreas at various ages. The percentage of TH$^+$ β-cells increased steadily during the growth phase (postnatal day 2 [P2]–2.5 months) and then stabilized (Fig. 4*A*). Immunostaining for replication markers Ki67 and pHH3 revealed that the TH$^+$ β-cells do replicate in neonatal life (Fig. 4*B–E*, Supplementary Fig. 4*A* and *B*). The percentage of replicating TH$^+$ β-cells was highly variable, likely due to their small number in the islets. In adult mice in which β-cells are typically quiescent but can replicate in response to increased insulin demand (36), several TH$^+$ β-cells were marked by the licensing factor Mcm2, which indicates replication competence (Supplementary Fig. 4*C* and *D*). The ability of TH$^+$ β-cells to replicate suggested these cells may not be senescent. Quantification of key senescence markers such as the presence of p21, p16, γ-H2AX, and SA-β-gal, and loss of LaminB1 (37,38) revealed that TH$^+$ β-cells are nonsenescent (Fig. 4*F–M*, Supplementary Fig. 4*E–R*). Moreover, none of the key senescence pathway genes were upregulated in the TH$^+$ β-cells in our scRNA-seq meta-analysis (Supplementary Fig. 4*S*). These data show that TH$^+$ β-cells can replicate and are not senescent under homeostatic conditions.

Th Promoter Is Methylated During the Transition From Endocrine Progenitors to β-Cells

DNA methylation patterning is a key mechanism that directs the establishment of pancreatic endocrine identity (6,8). We hypothesized that promoter methylation restricts TH expression to a select subset of β-cells, and we examined *Th* promoter methylation at different stages of endocrine

and comparison of each category between the TH$^+$ and TH$^-$ β-cells (*J*). *A, B, D–H*: Representative images from adult (aged 2 months) C57BL/6J mice (n = 5 mice); at least 25 independent images per pancreas were acquired. *C*: Data from 11 and 8 C57BL/6J pups at P5 and P21, respectively. *I* and *J*: Average distribution (*I*) and individual (*J*) data from four mice, with each point in *I* representing data from individual mice. Error bars show SEM. *$P < 0.05$, **$P < 0.01$, ***$P < 0.005$ by two-tailed Student t test (*C*) and one-way ANOVA with Fisher least significant difference test for (*J*). Scale bars: 50 μm.

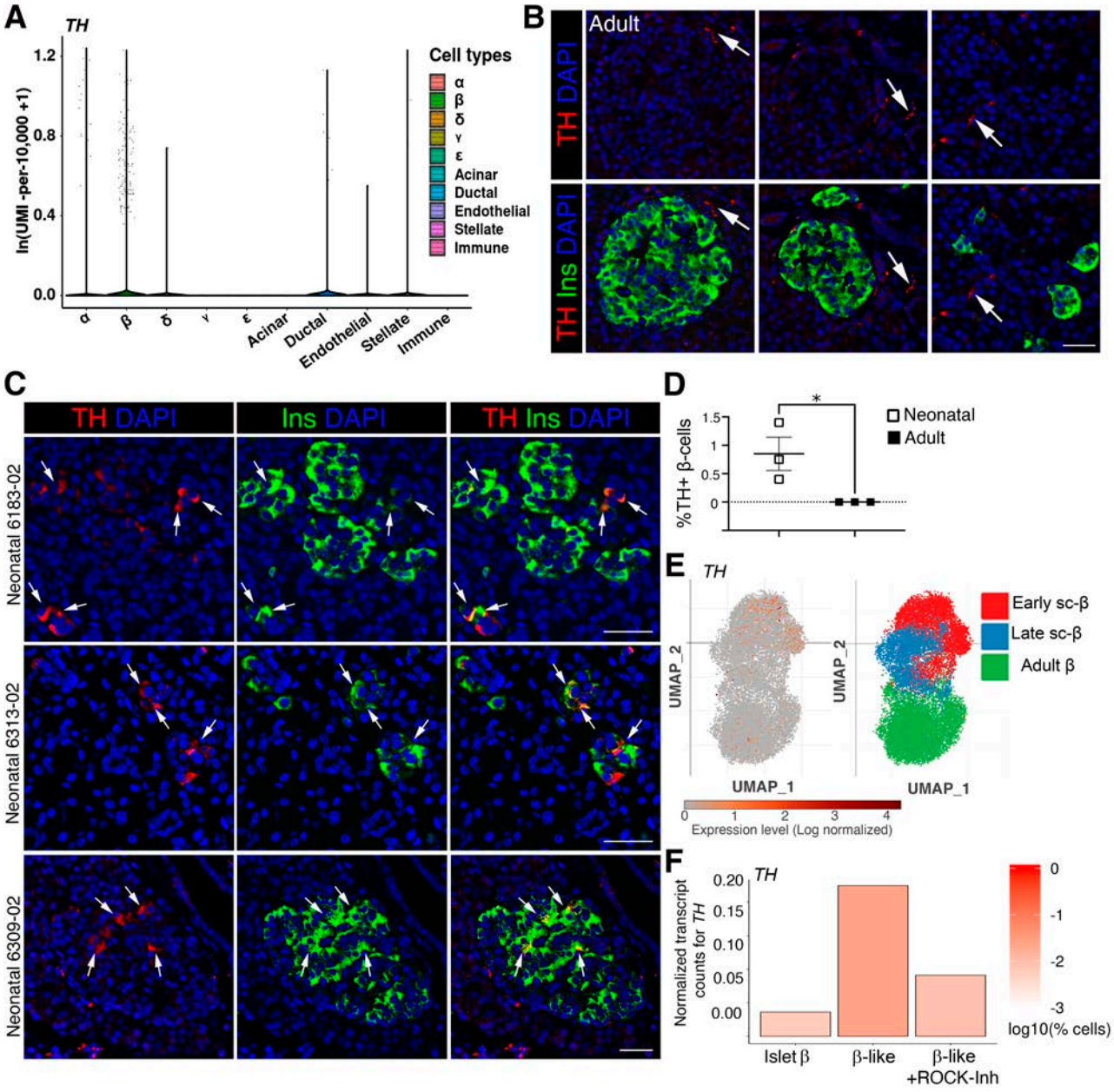

Figure 2— Developing human pancreas contains TH$^+$ β-cells. *A*: A violin plot of *TH* mRNA expression data in different endocrine cell populations generated from publicly accessible scRNA-seq data (27) hosted at the authors' website (https://powersbrissovalab.shinyapps.io/scRNAseq-Islets/#). *B*: Immunostaining for TH (red), insulin (Ins) (green), and DAPI (blue) in adult human pancreas (n = 3), showing islets of different sizes. A minimum of 30 images covering the entire pancreas section were acquired. *C*: Immunofluorescence images from three neonatal human pancreata showing TH (red), Ins (green), and DAPI (blue). Arrows indicate TH$^+$ β-cells. *D*: Quantification of TH$^+$ β-cells in neonatal and adult human pancreatic tissue (n = 3); 2,000 β-cells per sample were counted. *E*: A Uniform Manifold Approximation and Projection (UMAP) plot showing the distribution of *TH* expression in early and late human stem cell–derived β-cells (sc-β) and adult β-cells. Plot generated from a publicly accessible data set (30) hosted at (https://singlecell.broadinstitute.org/). *F*: Bar graph output of a β-Cell Hub (28,29) query showing normalized transcripts counts for *TH* in islet-derived or human stem cell–derived β-like cells, without or with ROCK inhibitor treatment (islet-β, β-like, and β-like plus ROCK-Inh, respectively). The β-Cell Hub is hosted at https://hiview.case.edu/public/BetaCellHub/versusisletResult.php. Error bars show SEM. *$P < 0.05$ by two-tailed Student t test (*D*). Scale bars: 50 μm. Inh, inhibitor; UMI, unique molecular identifier.

differentiation. We performed bisulfite sequencing for the *Th* promoter in pancreatic progenitors (Pdx1$^+$), endocrine progenitors (Neurogenin3 [Ngn3$^+$]), and β-cells (insulin$^+$) isolated from pancreatic tissue using lineage reporter mice at E11.5 (*Pdx1*-Cre:*R26R-YFP*), E13.5 (*Ngn3*-Cre:*R26R-YFP*), and E18.5 (*Ins1*-Cre^{Thor}:*R26R-YFP*), respectively. We found stage-specific, differential DNA methylation at the −2K region of the *Th* promoter, with the promoter being hypomethylated in the pancreatic and endocrine progenitors and hypermethylated in β-cells (Fig. 5*A*). No differences in DNA

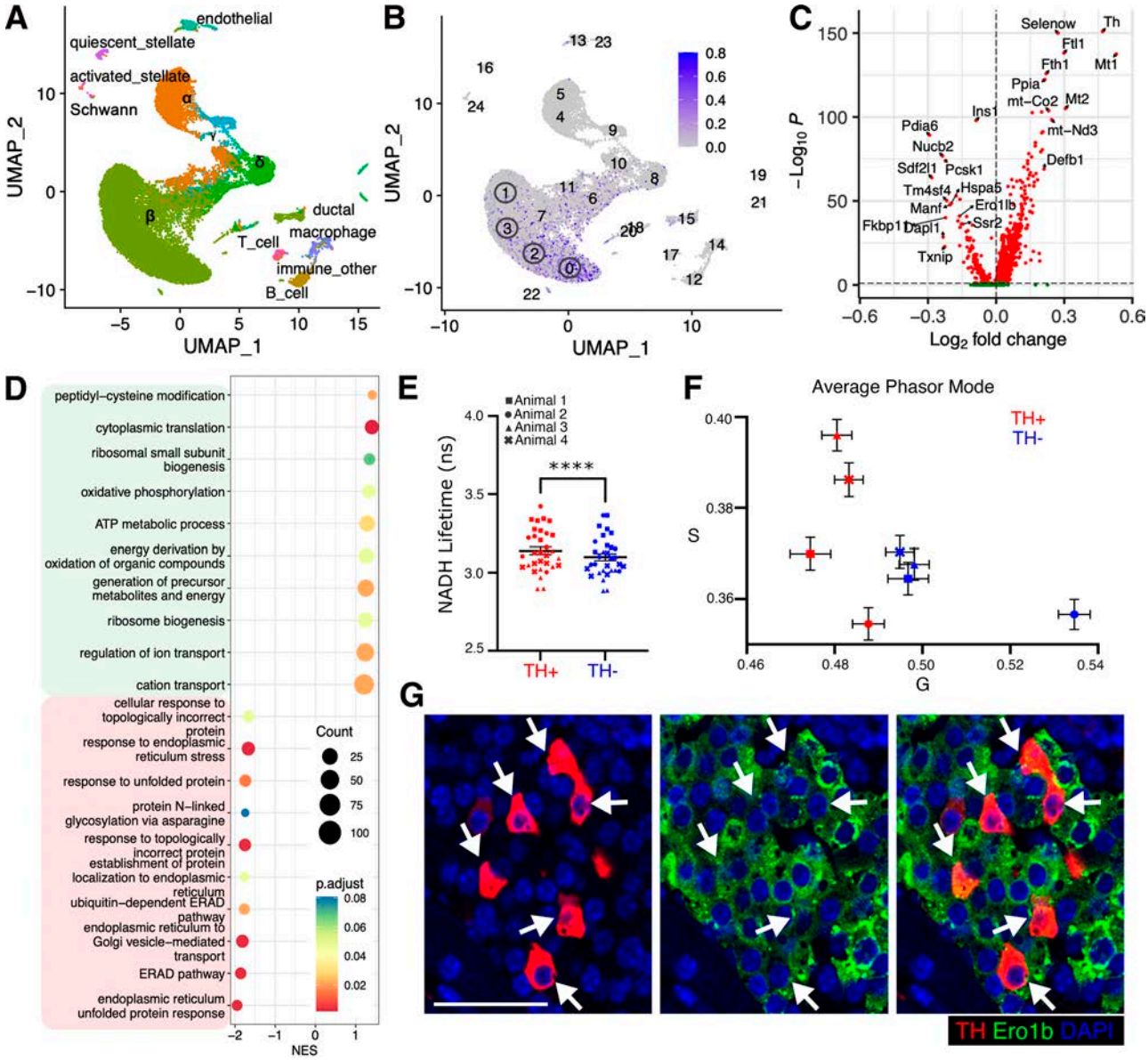

Figure 3—TH$^+$ β-cells display distinct molecular and metabolic characteristics. *A*: Analysis of scRNA-seq of mouse pancreatic islets from adult C57BL/6J mice fed regular chow. A Uniform Manifold Approximation and Projection (UMAP) plot is shown with individual cell types marked with specific colors. *B*: Distribution of *Th* expression within β-cell subtypes. The four major β-cell clusters (0–3) are marked by open circles. *C*: Volcano plot showing DEGs between *Th*$^+$ and *Th*$^-$ cells in all β-cell clusters. *D*: Gene-set enrichment analysis of the differentially expressed genes showing top enriched pathways for *Th*$^+$ vs. *Th*$^-$ cells in β-cell clusters. The up- and downregulated pathways are noted in top (light green) and bottom (light red) boxes. Enrichment was calculated for Gene Ontology Biological Process terms. *E*: NADH lifetime signatures for individual islets from each animal plotted for TH$^+$ (red) vs. TH$^-$ (blue) β-cells. Different symbols indicate data points from each animal. *F*: Lifetime modes for single islets were transformed onto phasor plots and averaged for each individual pancreas. Modes of phasor plot for TH$^+$ (red) vs. TH$^-$ (blue) for each individual animal (n = 8 islets/mouse, n = 4 mice) were plotted onto a *G* vs. *S* graph (arbitrary units). *G*: Representative immunofluorescence images for TH (red), Erol1b (green), and DAPI (blue) in pancreata from 2-month-old C57BL/6J mice (n = 5 mice, n = 25 images acquired per mouse sample). Arrows mark TH$^+$ cells. *A–D*: Meta-analysis of pooled scRNA-seq data from three independent islet preparations from 9-week-old C57BL/6J mice fed a regular diet. Error bars show SEM. ****$P < 0.001$ by paired t test (*E*). Scale bar: 50 μm. NES, normalized enrichment score; p.adjust, adjusted P value.

methylation were found in the other CG-rich regions in the promoter (Supplementary Fig. 5*A* and *B*).

This differential methylation was not due to stage-specific expression of Dnmt3a (the only de novo Dnmt present in endocrine lineage) (9), because Dnmt3a was expressed in the progenitors as well as β-cells (Fig. 5*B–D*). ChIP for Dnmt3a at the −2K region of the *Th* promoter revealed higher enrichment of Dnmt3a in the endocrine progenitors compared with pancreatic progenitors and β-cells (Fig. 5*E*). Expression analysis revealed very little overlap of Pdx1 and TH at E12.5 except for a rare few TH$^+$ cells marked by very low Pdx1, whereas none of

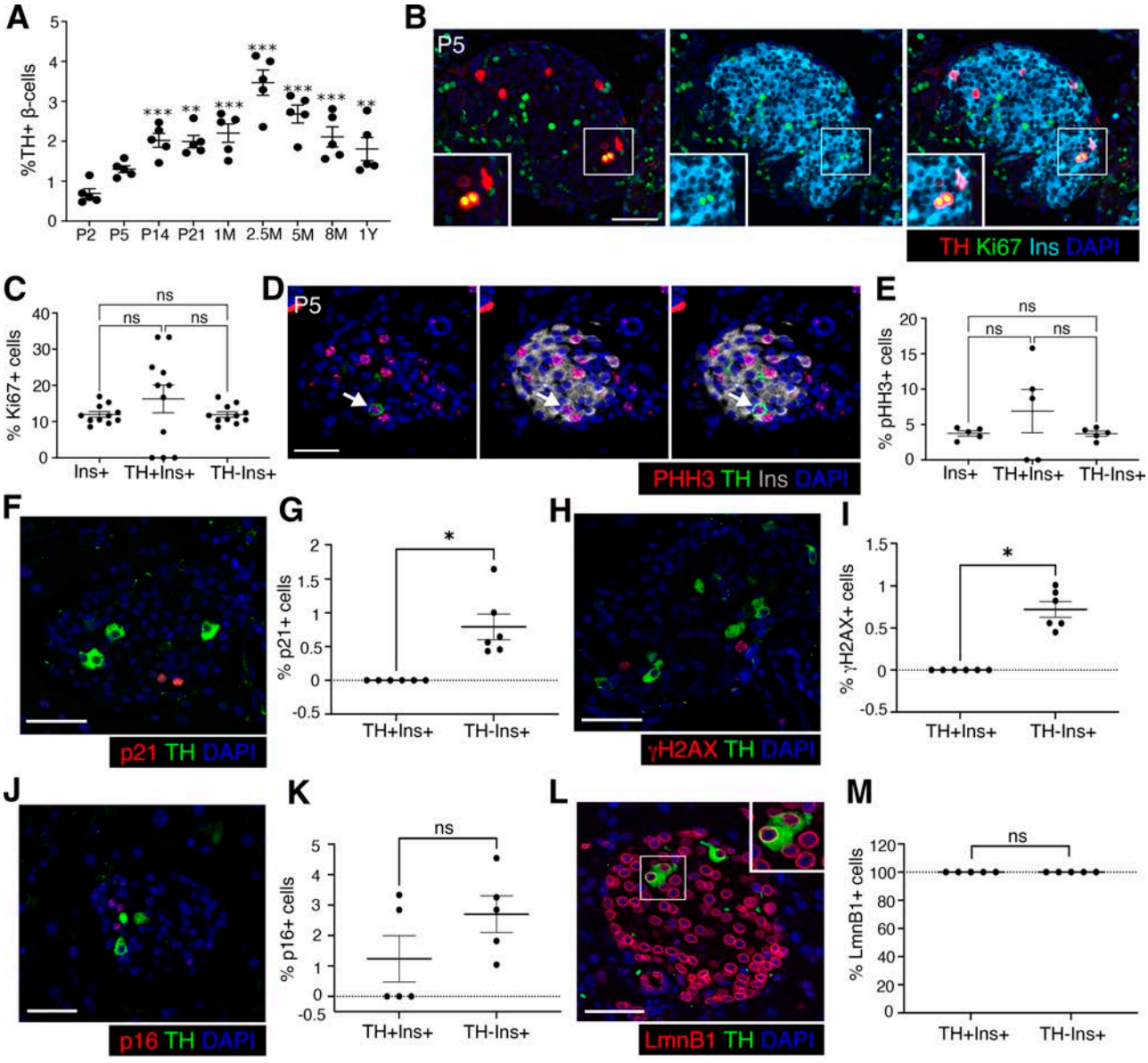

Figure 4—The TH^+ β-cells can replicate in postnatal life and are not senescent. We analyzed and quantified markers of replication (namely Ki67, pHH3) and senescence (namely, presence of p21, γH2AX, p16, and absence of LaminB1) in TH^+ and TH^- β-cells. *A*: Quantification of TH^+ β-cells shown as percentage of total β-cells at indicated stages in postnatal life (n = 5 mice/group; n = 700 β-cells/pancreas for P2–14; n = 1,500 β-cells per pancreas for P21 to 1 month; and n = 2,000 β-cells per pancreas for 2.5 months to 1 year). *P* values shown are compared with P2. *B* and *C*: Immunostaining (*B*) and quantification of specimens from 11 pups at P5 (*C*) for Ki67 (green), TH (red), insulin (Ins) (cyan), with DAPI (blue) in total, TH^+, and TH^- β-cells. Insets in *B* show a ×2 view of the areas marked by white boxes. β-Cells (n = 700/slide), two slides spanning 100 μm for each pancreas, n = 11 pups. *D* and *E*: Immunofluorescence labeling (*D*) and quantification from five pups at P5 (*E*) for phospho-histone H3 (pHH3; red) with Ins (gray), TH (green), DAPI (blue) in total, TH^+, and TH^- β-cells. β-Cells (n = 700/slide), two slides spanning 100 μm for each pancreas, n = 5 pups. *F* and *G*: Immunostaining (*F*) and quantification (n = 6 mice, 2 months old) (*G*) for p21 (red) and TH (green), with DAPI (blue) in TH^+, and TH^- β-cells. *H* and *I*: Immunofluorescence (*H*) and quantification (n = 6 mice, 2 months old) (*I*) for γH2AX (red) and TH (green), with DAPI (blue) in TH^+, and TH^- β-cells. *J* and *K*: Immunostaining (*J*) and quantification (n = 5 mice, 2 months old) (*K*) for p16 (red) and TH (green), with DAPI (blue) in TH^+, and TH^- β-cells. *L* and *M*: Immunofluorescence (*L*) and quantification (n = 5 mice, 2 months old) (*M*) for LaminB1 (LmnB1; red) and TH (green), with DAPI (blue) in TH^+, and TH^- β-cells. LmnB1 marks nuclear membrane in nonsenescent cells and should be absent from senescent cells. Inset in *L* shows a ×2 view of the areas marked by white boxes. All data are from wild-type C57BL/6J mice. Panels show representative confocal images (from at least 25 islet fields acquired) or mean data from indicated sample sizes with at least five mice per group at indicated ages. *G* and *I*: β-Cells (n = 2,000/slide were counted, two slides spanning 100 μm for each pancreas, n = 6 mice. *L* and *M*: A similar number of cells and slides were counted in five pups. Error bars show SEM. $*P < 0.05$, $**P < 0.01$, $***P < 0.005$ by one-way ANOVA with Bonferroni post hoc test (*A*, *C*, and *E*) and paired *t* test (*G*, *I*, *K*, and *M*). Scale bars: 50 μm.

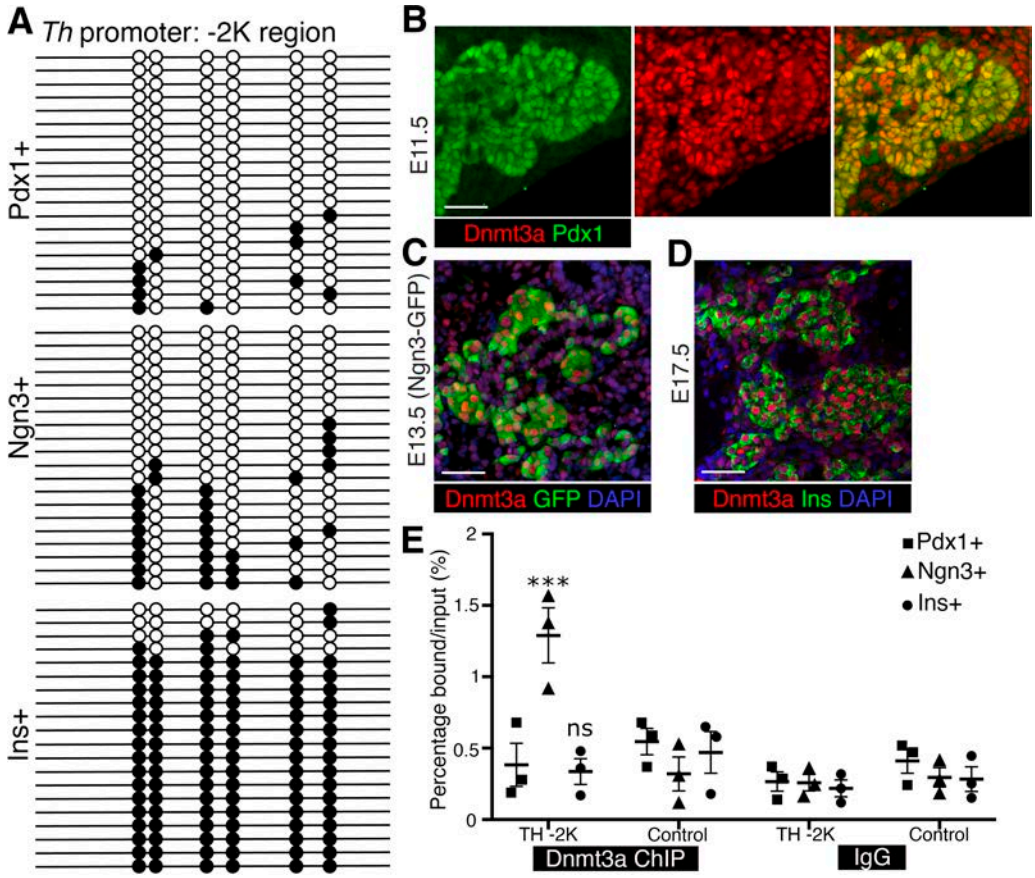

Figure 5—*Th* promoter undergoes Dnmt3a-dependent methylation during endocrine progenitor to β-cell differentiation. *A*: Bisulfite sequencing analysis of the *Th* promoter −2K region in purified mouse embryonic pancreatic progenitors, endocrine progenitors, and β-cells. Each line with dots is an independent clone; filled and open circles denote methylated and unmethylated CpGs, respectively. *B–D*: Representative immunostaining for Dnmt3a (red), with Pdx1 (green) at E11.5 (*B*), Ngn3-GFP (green) at E13.5 (*C*), and insulin (Ins) (green) at E17.5 (*D*), with DAPI in blue (*C* and *D*). *E*: ChIP analysis for Dnmt3a binding to the −2K region of the *Th* promoter or a negative control region in sorted pancreatic progenitors, endocrine progenitors, and β-cells, showing the percentage of bound DNA (over input) in Dnmt3a or control IgG immunoprecipitation. *A*: Representative data from one of three samples. *E*: Mean of three independent samples per group, each sample being a biological replicate pool of cells derived from multiple embryos, with error bars showing SEM. ***$P < 0.005$ by one-way ANOVA followed by a Bonferroni post hoc test. Scale bars: 50 μm.

the Ngn3$^+$ endocrine progenitors expressed TH at E13.5 (Supplementary Fig. 5*C* and *D*). Because TH was not expressed in the pancreatic or endocrine progenitors, the lack of promoter DNA methylation at these stages led us to determine the mechanism of *Th* repression at these stages. Histone H3–lysine 9 trimethylation (H3K9me3) creates a reversible repressive chromatin state prior to the establishment of the more stable DNA methylation (39). ChIP for H3K9me3 confirmed its enrichment at the −2K region of *Th* promoter in sorted pancreatic and endocrine progenitors (Supplementary Fig. 5*E*). These data show the stepwise establishment of repressive marks at the *Th* promoter through β-cell differentiation with DNA methylation as the final step and suggest a role for DNA methylation in restricting TH expression in differentiated β-cells.

Promoter DNA Methylation Is Essential for the Restriction of *Th* Expression in β-Cells

To establish a direct regulatory role of DNA methylation in restricting *Th* expression in β-cells during differentiation, we generated mice harboring loss of Dnmt3a in pancreatic, endocrine, and β-cell lineages and examined TH expression in the pancreas. Mice with Dnmt3a ablation in the pancreatic and endocrine progenitor lineages (*Pdx1*-Cre:*Dnmt3a*$^{fl/fl}$ [3aPancKO] and *Ngn3*-Cre:*Dnmt3a*$^{fl/fl}$ [3aEndoKO], respectively) showed an ∼16-fold increase in the number of TH$^+$ β-cells. Loss of Dnmt3a in the β-cell lineage (*Ins1*-Cre^{Thor}:*Dnmt3a*$^{fl/fl}$ [3aBetaKO]) did not alter the number of TH$^+$ β-cells (Fig. 6*A–F*, Supplementary Fig. 6*A–C*). We confirmed the efficiency of recombination and Dnmt3a ablation by Cre-driven fluorescent protein expression and Dnmt3a immunostaining (Supplementary Fig. 6*A–H*). We chose neonatal stages to confirm Dnmt3a ablation because its levels decline dramatically after weaning (9). The changes in β-cell identity upon Dnmt3a ablation did not involve any changes in β-cell mass but were accompanied by blunting of GSIS (Supplementary Fig. 6*I* and *J*). Additionally, Dnmt3a ablation in the progenitors led to loss of TH restriction in δ- but not α-cells (Supplementary Fig. 6*K–N*). In agreement with the changes in TH expression, the −2K region of the *Th* promoter was

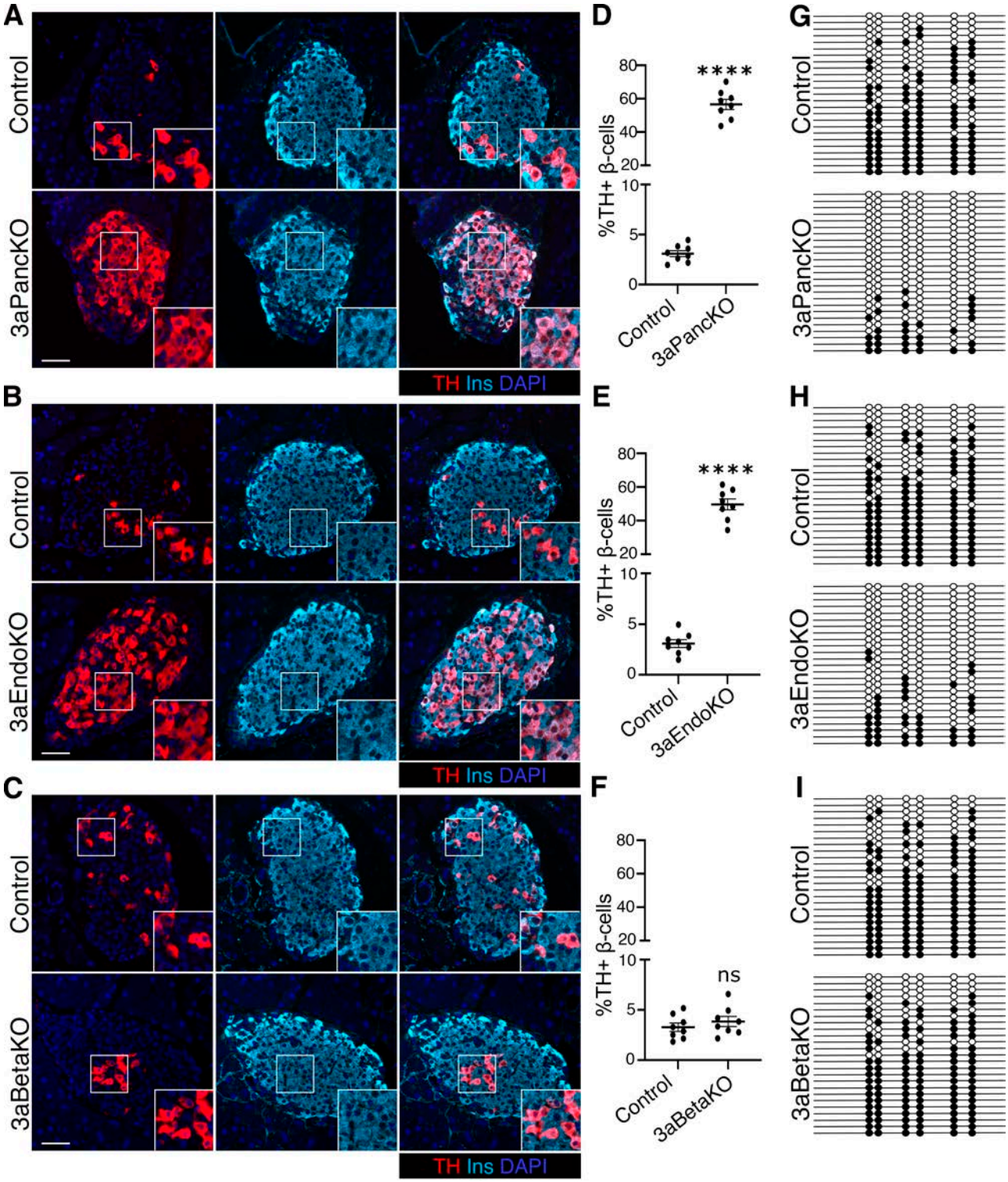

Figure 6— Dnmt3a ablation in progenitors, but not β-cells, leads to *Th* promoter demethylation and dysregulation in β-cells. *A–F*: Representative images (chosen from at least 25 images per mouse pancreas, $n = 5$ mice) (*A–C*) and quantification of TH expression (*D–F*) in pancreatic sections from 2.5-month-old mice with Dnmt3a ablation at various stages of pancreas development and littermate controls. TH (red), insulin (Ins) (cyan), and DAPI (blue). Insets show a ×2 magnified view of areas marked by white boxes. β-Cells ($n = 2{,}500$/slide) were counted, two slides spanning 100 μm for each pancreas, $n = 8$ pancreas (mice). *G–I*: Bisulfite sequencing analysis of the *Th* promoter −2K region in islets from adult (2.5 months old) 3aPancKO, 3aEndoKO, and 3aBetaKO mice and corresponding littermate controls. Each horizontal line with dots represents an independent clone; 25 clones are shown here, with filled circles representing a methylated CpG and open circles denoting an unmethylated CpG residue. *A–C*: Examples from five independent samples. *D–F*: Mean data from eight mice per group, with error bars representing SEM. ****$P < 0.001$, determined by two-tailed Student *t* test. *G*, *H*, and *I*: Representative data for one of the five independent islet preparations from individual KO and control mice. Scale bars: 50 μm.

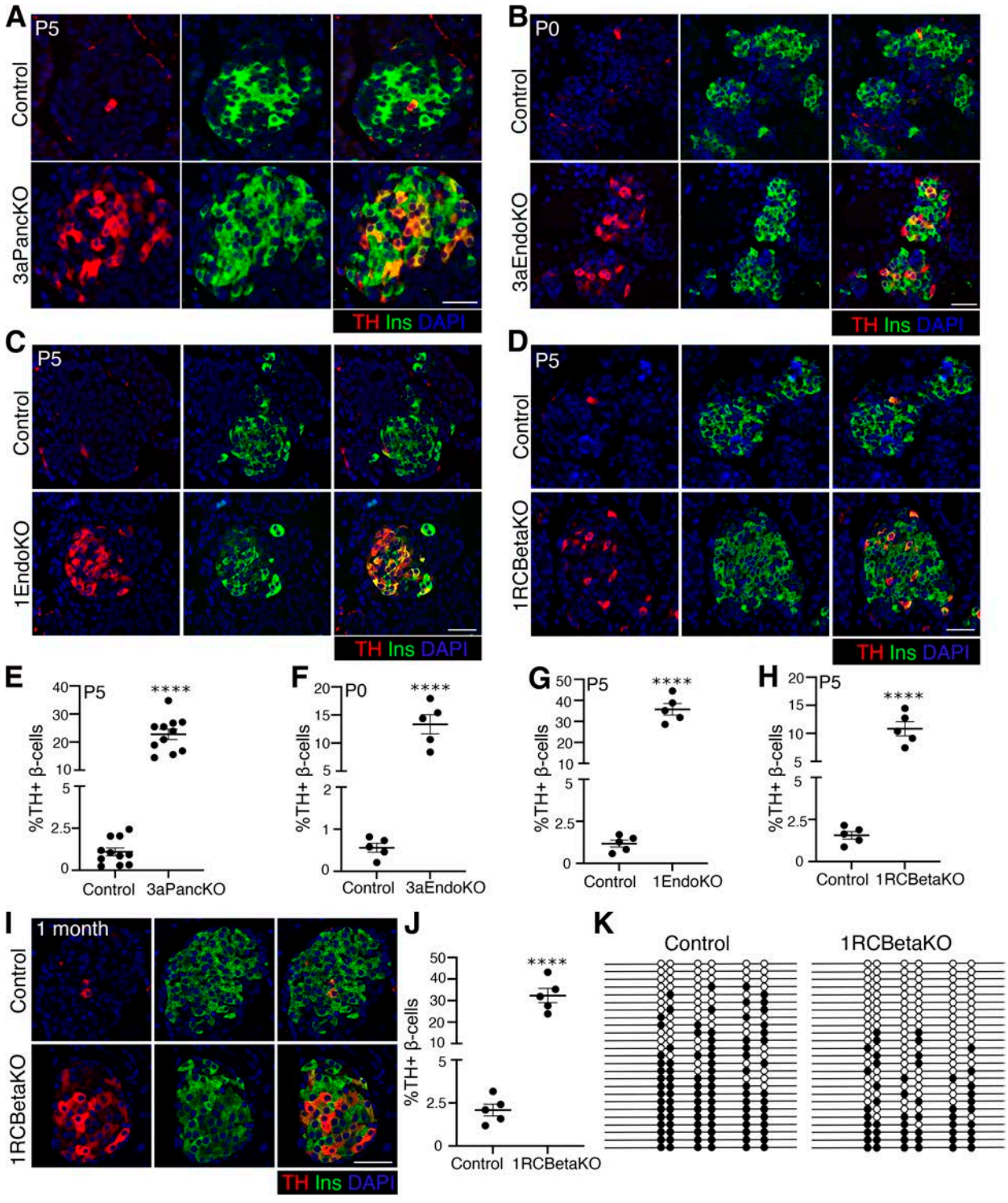

Figure 7— Dnmt3a-dependent restriction of *Th* expression occurs prior to β-cell maturation and needs to be maintained for its continued restriction. *A–H*: Immunofluorescence analysis (*A–D*) and quantification (*E–H*) of TH expression in pancreata from mice with Dnmt3a or Dnmt1 ablation in different lineages, along with littermate controls at indicated ages. TH (red), insulin (Ins) (green), and DAPI (blue). β-Cells ($n = 500$) counted per slide for P0, 700 β-cells counted per slide for P5, two slides spanning 80 μm for each pancreas; $n = 8$ pups in *E* and $n = 5$ pups for *F–H*. *I* and *J*: Immunostaining (*I*) and quantification (*J*) of TH in pancreata from 1-month-old mice with β-cell–specific Dnmt1 ablation (1RCBetaKO), and littermate controls. TH (red), Ins (green), and DAPI (blue). *K*: Bisulfite sequencing of the −2K region of *Th* locus in β-cells sorted from 1-month-old 1RCBetaKO and control mice. Each horizontal line with dots represents an independent clone, with 25 clones shown here. Filled circles represent a methylated CpG; open circles indicate an unmethylated CpG residue. *A–J*: Representative images (from at least 20 images acquired per sample) or mean data from eight samples for 3aPancKO and controls, and five for the other groups. *K*: Representative data for one of the three independent β-cell preparations from individual KO and control mice. Error bars show SEM. ****$P < 0.001$, determined by two-tailed Student *t* test. Scale bars: 50 μm.

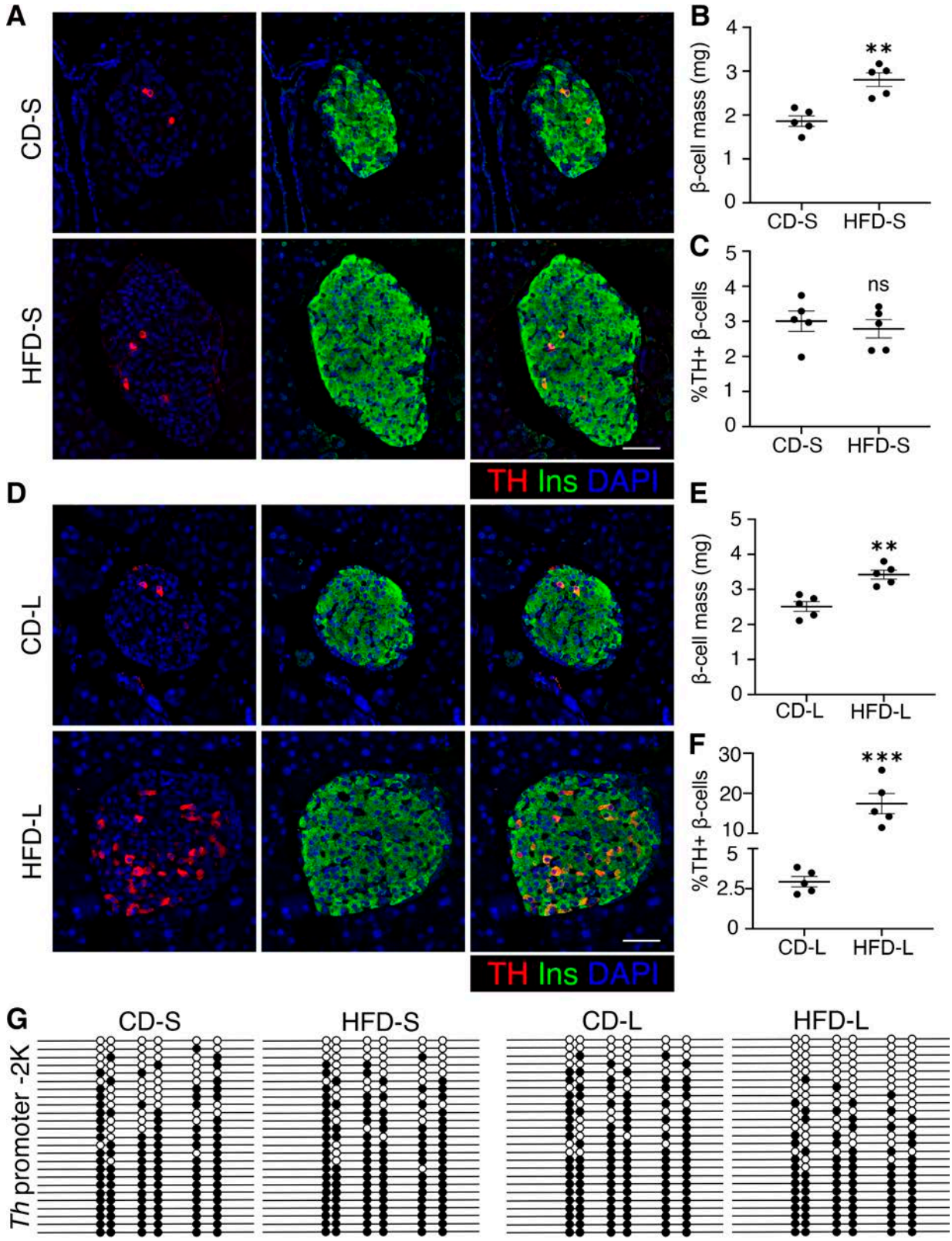

Figure 8—Chronic HFD leads to promoter demethylation–dependent dysregulation of *Th* expression in β-cells. *A–C*: Immunofluorescence for TH (red) and Ins (green), with DAPI in blue (*A*), β-cell mass (*B*), and quantification of TH^+ β-cells (*C*) in wild-type, 7-week-old mice fed a HFD or control diet for a short term (HFD-S or CD-S, respectively). *D–F*: Immunostaining for TH (red) insulin (green), and DAPI (blue) (*D*), β-cell mass (*E*), and quantification of TH^+ β-cells (*F*), in wild-type, 7-week-old mice fed an HFD or control diet for a long term (HFD-L or CD-L, respectively). Representative images shown are from at least 30 images acquired per pancreas sample. For quantification, 2,500 β-cells per slide were counted, two slides spanning 100 μm for each pancreas, $n = 5$ pancreas (mice). *G*: Bisulfite sequencing analysis of the *Th*

hypomethylated in islets from 3aPancKO and 3aEndoKO mice but not in 3aBetaKO islets (Fig. 6*D–I*). Thus, de novo methylation by Dnmt3a is required to restrict *Th* expression in differentiated β-cells.

DNA Methylation–Dependent *Th* Restriction Occurs Prior to β-Cell Maturation, and Maintenance of Methylation Is Required for Sustained TH Repression

Dnmt3a dependent de novo DNA methylation is essential for β-cell maturation (9). Thus, we tested if the DNA methylation–dependent restriction of *Th* in β-cells is linked to functional maturation. We compared TH^+ β-cells in 3aPancKO and control pancreas specimens at P0 and P5 before functional maturation. The increase in the number of TH^+ β-cells in the 3aPancKO was very pronounced at P5 and was evident even immediately after birth (Fig. 7*A* and *E*, Supplementary Fig. 7*A* and *B*). Dnmt3a ablation in the endocrine lineage showed a similar de-repression of TH in β-cells at P0 (Fig. 7*B* and *F*). To determine the developmental timeline of TH de-repression in the absence of Dnmt3a, we examined 3aPancKO, 3aEndoKO, and control tissue during late endocrine differentiation (E16.5) and observed an increase in TH^+ β-cells in the two KO models, even at this stage before functional maturation (Supplementary Fig. 7*C–F*).

Maintenance of the existing DNA methylation patterns through replication is essential for the preservation of β- versus α-cell identity in postnatal life (6). To determine if maintenance of promoter methylation is required for sustained *Th* restriction in β-cells, we generated mice lacking the maintenance methyltransferase Dnmt1 in endocrine and β-cell lineages (*Ngn3*-Cre:*Dnmt1*$^{fl/fl}$ [1EndoKO], and *RIP*-Cre^{Herr}:*Dnmt1*$^{fl/fl}$ [1RCBetaKO]). Because Dnmt1 depletion in β-cells results in their conversion to α-cells in late adult life (6), we focused our analysis on neonates and young adults (P5 to 1 month) before the onset of transdifferentiation to α-cells. We observed an increased number of TH^+ β-cells in the 1EndoKO and 1RCBetaKO mice at P5 (Fig. 7*C* and *D*), the increase being much higher in 1EndoKO, congruent with the timeline of *Th* promoter methylation (Fig. 7*G* and *H*). This increase was accompanied by loss of *Th* promoter methylation in β-cells harvested from 1-month-old 1RCBetaKO mice (Fig. 7*I–K*). These data show that propagation of *Th* promoter methylation is required to maintain β-cell heterogeneity.

Promoter Demethylation Dysregulates β-Cell TH Expression in Response to Chronic Overnutrition

Given the essential requirement of maintenance DNA methylation in restricting TH in β-cells, we asked if conditions that warrant β-cell expansion alter the proportion of TH^+ β-cells. A prior study had reported increased TH^+ β-cell numbers in genetically obese *ob/ob* mice that undergo β-cell expansion in young age. However, the increased number of TH^+ β-cells only occurred in the older *ob/ob* mice (10). Because there is no age-dependent increase in TH^+ β-cells in wild-type mice (Fig. 4*A*), we hypothesized that chronic increase in insulin demand because of insulin resistance was an underlying cause. To test this, young adult, wild-type mice (7 weeks old) were either exposed to a short-term (8 weeks) or long-term (16 weeks) HFD regimen or maintained on a CD. The two regimens are designed to model successful β-cell adaptation to increased demand for insulin (short-term HFD) or the subsequent decompensation as β-cell de-differentiation and failure ensue (40). As expected, both short- and long-term HFD led to increased body weight and impaired glucose tolerance (Supplementary Fig. 8*A–D*). Although end point analysis showed increased islet size and β-cell mass in mice fed the short- and long-term HFDs, only the long-term HFD regimen resulted in an increase in TH^+ β-cells (Fig. 8*A–F*) concomitant with impaired islet function (Supplementary Fig. 8E) that hallmarks β-cell decompensation in long-term HFD (41). This finding suggests that chronic β-cell workload due to persistently high insulin demand could disrupt the epigenetic restriction of TH in β-cells. Thus, we performed bisulfite sequencing analysis of *Th* promoter in islets from mice fed a short- and long-term HFD versus appropriate controls. We observed loss of promoter DNA methylation corresponding to increased *Th* mRNA expression in islets from mice fed the long-term but not short-term HFD (Fig. 8*G*, Supplementary Fig. 8*F* and *G*), indicating a failure to maintain DNA methylation upon chronically high insulin demand. This suggests that maintenance of epigenetic patterns is essential to preserve β-cell identity during adaptation and fails during β-cell decompensation.

DISCUSSION

Pancreatic β-cells share several features with neurons, including shared developmental transcriptional programs (42). Islet cells contain neurotransmitters that regulate insulin secretion and enzymes such as TH that regulate their synthesis (43,44). We observed TH expression in a small subpopulation of adult β-cells and rare δ-cells, suggesting that neuron-like features underlie heterogeneity of many endocrine cell types. Early endocrine precursors express specific neuronal markers whose expression gets restricted as endocrine identities are refined. Accordingly, it has been postulated that the TH^+ β-cells may indicate a developmentally immature precursor (45), which appears to be the

promoter −2K region in islets from mice fed an HFD or CD for 8 weeks (HFD-S, CD-S) or 16 weeks (HFD-L, CD-L). Each horizontal line with dots represents an independent clone; 25 clones are shown for each sample, with filled circles indicating methylated CpG and open circles indicating unmethylated CpG. Immunofluorescence data show representative images from five samples. The data on β-cell mass and TH^+ β-cell quantification are a mean of five independent samples per group, whereas the bisulfite-sequencing data are from representative clones from one of the three independent samples per group. Error bars show SEM of the mean. $^{**}P < 0.01$, $^{***}P < 0.005$ determined by two-tailed Student *t* test. Scale bars: 50 μm.

case in humans. Presence of TH in fetal and neonatal human pancreases and sc-β-cells, but not adult human pancreases, highlights a major developmental difference in *TH* regulation compared with mice. Recent studies have identified β-cells harboring serotonergic markers in human sc-β-cell differentiation (46). This finding suggests that expression of neuron-like features characterize sc-β-cells, revealing a bottleneck in generating mature human sc-β-cells.

We show that DNA methylation is essential for regulating endocrine identity and heterogeneity in homeostatic and stress conditions. The specification and maintenance of cell fates require the precise temporal orchestration of epigenetic patterns to regulate stage-specific transcriptional programs (3). De novo DNA methylation is essential for β-cell lineage specification and functional maturation in fetal and early postnatal life. Maintenance of these methylation patterns by Dnmt1 allows the continued restriction of α-cell fate to preserve β-cell identity in postnatal life (6,8,9). We establish that the de novo DNA methylation–dependent restriction of TH expression in β-cells occurs during lineage specification prior to their functional maturation. Heterogeneity of Dnmt expression within the endocrine progenitor pool dictates their lineage commitment bias (7); similar mechanisms might be involved in limiting TH expression to a select few β-cells. The ablation of *Dnmt1* in endocrine progenitors and β-cells results in the ectopic TH expression in β-cells prior to their trans-differentiation to α-cells. These temporal changes in β-cell identity upon the loss of maintenance methylation suggest differences in the stringency of restriction between cell fates with different degrees of relatedness. It is likely that the epigenetic barriers between different β-cell subtypes are more plastic than those between β- and α-cells. DNA methylation plays distinct regulatory roles in different endocrine lineages, whereas loss of Dnmt1 in β-cells results in their conversion to α-cells; Dnmt1 ablation in α- or δ-cells does not convert them to β-cells (6,47,48). The dysregulation of *Th* in β- and δ-cells, but not α-cells, upon Dnmt ablation further highlights the lineage specificity of DNA methylation regulation.

It has been suggested that TH^+ islet cells may be senescent (10). We show that TH^+ β-cells do replicate during the neonatal growth phase and do not harbor senescence markers under homeostatic conditions. Instead, these cells bear signatures of overactive protein synthesis, poor ER stress response, and higher OxPhos, hallmarks of β-cells predisposed to ER and oxidative stress (49). We also show that conditions of β-cell decompensation can disrupt the epigenetic repression of the *Th* promoter and alter β-cell identity, marked by an increase in TH^+ β-cell numbers. These data explain prior observations of increased TH^+ β-cell numbers in older, genetically obese *ob/ob* mice without any accompanying replication (10). The older *ob/ob* mice represent a β-cell decompensation state in response to chronically elevated insulin demand, where β-cell replication does not occur (40). Accumulation of these cells during β-cell decompensation, along with the inverse correlation between TH^+ β-cell abundance and islet function (12), suggests the possibility of β-cells de-differentiating into a TH^+ state and acquiring a dysfunctional phenotype. The large-scale changes in human islet methylome associated with β-cell identity and function genes in type 2 diabetes strengthen this idea (50). Our data suggest that embryonic DNA-methylation patterning may affect postnatal β-cell identity, which is noteworthy, given that over- or undernutrition during development can predispose to risk of β-cell failure (4). Future work will identify the specific aspects of postnatal β-cell phenotype that rely upon embryonic epigenetic patterning and will elucidate the significance of such a paradigm.

Acknowledgments. The authors thank Alexander Ham, Giovanni Hernandez-De La Peña, and Pope Rodnoi (S.D. Laboratory) for technical support; Dr. Rachel Steward and Family Planning Associates for the (fetal) tissue donation (Children's Hospital Los Angeles tissue repository); and Drs. Jason Junge and Peiyu Wang (University of Southern California) for expertise and consultation in FLIM studies. The authors thank Dr. David Ron (University of Cambridge) and Dr. Mark Huising (University of California, Davis) for the gifts of Ero1b and Ucn3 antibodies, respectively.

Funding. This work was supported by the National Institute of Diabetes and Digestive and Kidney Diseases (NIDDK; grants R01DK120523 to S.D., R01DK119590 to H.-P.S., and 1R01DK133504 to S.K.G.), the Human Islet Research Network (a New Investigator Award to S.D. via NIDDK grant UC4DK104162), the Homer & Gloria Harvey Family Foundation, the Paul Lester Foundation, and the Saban Research Institute (to S.K.G.). Work in the S.D. and H.-P.S. laboratories is also supported by City of Hope (start-up support to S.D. and H.-P.S.), the Wanek Family Foundation to Cure Type 1 Diabetes (S.D. and H.-P.S.), and theLions Club Initiative (S.D.).

Duality of Interest. No potential conflicts of interest relevant to this article were reported.

Author Contributions. S.K.G. and S.D. conceived and planned the study. N.P., J.K.W., J.C., M.S.R., S.K.G., and S.D. performed the experiments. N.P., J.K.W., S.B., J.C., M.S.R., A.E.B., X.W., S.K.G., and S.D. performed the analyses. N.P., J.K.W., S.B., J.C., A.E.B., X.W., H.-P.S., S.K.G., and S.D. interpreted data. N.P., S.B., X.W., H.-P.S., S.K.G., and S.D. wrote the manuscript. H.-P.S., S.K.G., and S.D. acquired funding. S.D. is the guarantor of this work and, as such, had full access to all the data in the study and takes responsibility for the integrity of the data and the accuracy of the data analysis.

Prior Presentation. Part of this work was presented at the American Diabetes Association 79th Scientific Sessions, San Francisco, CA, 7–11 June 2019, and the American Diabetes Association 82nd Scientific Sessions, New Orleans, LA, 3–7 June 2022.

References

1. Benninger RKP, Kravets V. The physiological role of β-cell heterogeneity in pancreatic islet function. Nat Rev Endocrinol 2022;18:9–22

2. Gutierrez GD, Gromada J, Sussel L. Heterogeneity of the pancreatic beta cell. Front Genet 2017;8:22

3. Avrahami D, Kaestner KH. Epigenetic regulation of pancreas development and function. Semin Cell Dev Biol 2012;23:693–700

4. Parveen N, Dhawan S. DNA methylation patterning and the regulation of beta cell homeostasis. Front Endocrinol (Lausanne) 2021;12:651258

5. Georgia S, Kanji M, Bhushan A. DNMT1 represses p53 to maintain progenitor cell survival during pancreatic organogenesis. Genes Dev 2013;27:372–377

6. Dhawan S, Georgia S, Tschen SI, Fan G, Bhushan A. Pancreatic β cell identity is maintained by DNA methylation-mediated repression of Arx. Dev Cell 2011;20:419–429

7. Liu J, Banerjee A, Herring CA, et al. Neurog3-independent methylation is the earliest detectable mark distinguishing pancreatic progenitor identity. Dev Cell 2019;48:49–63.e7
8. Papizan JB, Singer RA, Tschen SI, et al. Nkx2.2 repressor complex regulates islet β-cell specification and prevents β-to-α-cell reprogramming. Genes Dev 2011;25:2291–2305
9. Dhawan S, Tschen SI, Zeng C, et al. DNA methylation directs functional maturation of pancreatic β cells. J Clin Invest 2015;125:2851–2860
10. Teitelman G, Alpert S, Hanahan D. Proliferation, senescence, and neoplastic progression of beta cells in hyperplasic pancreatic islets. Cell 1988;52:97–105
11. Morrow LA, Morganroth GS, Herman WH, Bergman RN, Halter JB. Effects of epinephrine on insulin secretion and action in humans. Interaction with aging. Diabetes 1993;42:307–315
12. Mitok KA, Freiberger EC, Schueler KL, et al. Islet proteomics reveals genetic variation in dopamine production resulting in altered insulin secretion. J Biol Chem 2018;293:5860–5877
13. Jackson-Grusby L, Beard C, Possemato R, et al. Loss of genomic methylation causes p53-dependent apoptosis and epigenetic deregulation. Nat Genet 2001;27:31–39
14. Kaneda M, Okano M, Hata K, et al. Essential role for de novo DNA methyltransferase Dnmt3a in paternal and maternal imprinting. Nature 2004;429: 900–903
15. Hingorani SR, Petricoin EF, Maitra A, et al. Preinvasive and invasive ductal pancreatic cancer and its early detection in the mouse. Cancer Cell 2003;4:437–450
16. Schonhoff SE, Giel-Moloney M, Leiter AB. Neurogenin 3-expressing progenitor cells in the gastrointestinal tract differentiate into both endocrine and non-endocrine cell types. Dev Biol 2004;270:443–454
17. Thorens B, Tarussio D, Maestro MA, Rovira M, Heikkilä E, Ferrer J. Ins1(Cre) knock-in mice for beta cell-specific gene recombination. Diabetologia 2015;58:558–565
18. Soriano P. Generalized lacZ expression with the ROSA26 Cre reporter strain. Nat Genet 1999;21:70–71
19. Lee CS, Perreault N, Brestelli JE, Kaestner KH. Neurogenin 3 is essential for the proper specification of gastric enteroendocrine cells and the maintenance of gastric epithelial cell identity. Genes Dev 2002;16:1488–1497
20. Hara M, Wang X, Kawamura T, et al. Transgenic mice with green fluorescent protein-labeled pancreatic beta -cells. Am J Physiol Endocrinol Metab 2003;284:E177–E183
21. Tschen SI, Dhawan S, Gurlo T, Bhushan A. Age-dependent decline in beta-cell proliferation restricts the capacity of beta-cell regeneration in mice. Diabetes 2009;58:1312–1320
22. Rodnoi P, Rajkumar M, Moin ASM, Georgia SK, Butler AE, Dhawan S. Neuropeptide Y expression marks partially differentiated β cells in mice and humans. JCI Insight 2017;2:e94005
23. Piñeros AR, Gao H, Wu W, Liu Y, Tersey SA, Mirmira RG. Single-cell transcriptional profiling of mouse islets following short-term obesogenic dietary intervention. Metabolites 2020;10:513
24. Teitelman G, Alpert S, Polak JM, Martinez A, Hanahan D. Precursor cells of mouse endocrine pancreas coexpress insulin, glucagon and the neuronal proteins tyrosine hydroxylase and neuropeptide Y, but not pancreatic polypeptide. Development 1993;118:1031–1039
25. Reinert RB, Cai Q, Hong JY, et al. Vascular endothelial growth factor coordinates islet innervation via vascular scaffolding. Development 2014;141:1480–1491
26. Mawla AM, Huising MO. Navigating the depths and avoiding the shallows of pancreatic islet cell transcriptomes. Diabetes 2019;68:1380–1393
27. Shrestha S, Saunders DC, Walker JT, et al. Combinatorial transcription factor profiles predict mature and functional human islet α and β cells. JCI Insight 2021;6:e151621
28. Weng C, Xi J, Li H, et al. Single-cell lineage analysis reveals extensive multimodal transcriptional control during directed beta-cell differentiation. Nat Metab 2020;2:1443–1458
29. Balboa D, Barsby T, Lithovius V, et al. Functional, metabolic and transcriptional maturation of human pancreatic islets derived from stem cells. Nat Biotechnol 2022;40:1042–1055
30. Ghazizadeh Z, Kao DI, Amin S, et al. ROCKII inhibition promotes the maturation of human pancreatic beta-like cells. Nat Commun 2017;8:298
31. Millette K, Cuala J, Wang P, et al. SARS-CoV2 infects pancreatic beta cells in vivo and induces cellular and subcellular disruptions that reflect beta cell dysfunction. 20 July 2021 [preprint] Res Sq:rs.3.rs-592374. doi: 10.21203/rs.3.rs-592374/v1.
32. Lakowicz JR, Szmacinski H, Nowaczyk K, Johnson ML. Fluorescence lifetime imaging of free and protein-bound NADH. Proc Natl Acad Sci USA 1992;89:1271–1275
33. Zito E, Chin KT, Blais J, Harding HP, Ron D. ERO1-beta, a pancreas-specific disulfide oxidase, promotes insulin biogenesis and glucose homeostasis. J Cell Biol 2010;188:821–832
34. Khoo C, Yang J, Rajpal G, et al. Endoplasmic reticulum oxidoreductin-1-like β (ERO1lβ) regulates susceptibility to endoplasmic reticulum stress and is induced by insulin flux in β-cells. Endocrinology 2011;152:2599–2608
35. Georgia S, Bhushan A. Beta cell replication is the primary mechanism for maintaining postnatal beta cell mass. J Clin Invest 2004;114:963–968
36. Dhawan S, Georgia S, Bhushan A. Formation and regeneration of the endocrine pancreas. Curr Opin Cell Biol 2007;19:634–645
37. Thompson PJ, Shah A, Ntranos V, Van Gool F, Atkinson M, Bhushan A. Targeted elimination of senescent beta cells prevents type 1 diabetes. Cell Metab 2019;29:1045–1060.e10
38. Walker EM, Cha J, Tong X, et al. Sex-biased islet β cell dysfunction is caused by the MODY MAFA S64F variant by inducing premature aging and senescence in males. Cell Rep 2021;37:109813
39. Lehnertz B, Ueda Y, Derijck AA, et al. Suv39h-mediated histone H3 lysine 9 methylation directs DNA methylation to major satellite repeats at pericentric heterochromatin. Curr Biol 2003;13:1192–1200
40. Weir GC, Bonner-Weir S. Five stages of evolving beta-cell dysfunction during progression to diabetes. Diabetes 2004;53(Suppl. 3):S16–S21
41. Gupta D, Jetton TL, LaRock K, et al. Temporal characterization of β cell-adaptive and -maladaptive mechanisms during chronic high-fat feeding in C57BL/6NTac mice. J Biol Chem 2017;292:12449–12459
42. Eberhard D. Neuron and beta-cell evolution: learning about neurons is learning about beta-cells. BioEssays 2013;35:584
43. Iturriza FC, Thibault J. Immunohistochemical investigation of tyrosine-hydroxylase in the islets of Langerhans of adult mice, rats and guinea pigs. Neuroendocrinology 1993;57:476–480
44. Rodriguez-Diaz R, Dando R, Jacques-Silva MC, et al. Alpha cells secrete acetylcholine as a non-neuronal paracrine signal priming beta cell function in humans. Nat Med 2011;17:888–892
45. Teitelman G, Lee JK. Cell lineage analysis of pancreatic islet development: glucagon and insulin cells arise from catecholaminergic precursors present in the pancreatic duct. Dev Biol 1987;121:454–466
46. Veres A, Faust AL, Bushnell HL, et al. Charting cellular identity during human in vitro β-cell differentiation. Nature 2019;569:368–373
47. Chakravarthy H, Gu X, Enge M, et al. Converting adult pancreatic islet α cells into β cells by targeting both Dnmt1 and Arx. Cell Metab 2017;25: 622–634
48. Damond N, Thorel F, Kim SK, Herrera PL. Dnmt1 activity is dispensable in δ-cells but is essential for α-cell homeostasis. Int J Biochem Cell Biol 2017;88:226–235
49. Sharma RB, Landa-Galván HV, Alonso LC. Living dangerously: protective and harmful ER stress responses in pancreatic β-cells. Diabetes 2021;70: 2431–2443
50. Volkmar M, Dedeurwaerder S, Cunha DA, et al. DNA methylation profiling identifies epigenetic dysregulation in pancreatic islets from type 2 diabetic patients. EMBO J 2012;31:1405–1426